NANO EXPRESS　　　　　　　　　　　　　　　　　　**Open Access**

Fabrication of TiN nanostructure as a hydrogen peroxide sensor by oblique angle deposition

Zheng Xie[1,2], Xiangxuan Liu[2], Weipeng Wang[1], Can Liu[1], Zhengcao Li[1] and Zhengjun Zhang[3*]

Abstract

Nanostructured titanium nitride (TiN) films with varying porosity were prepared by the oblique angle deposition technique (OAD). The porosity of films increases as the deposition angle becomes larger. The film obtained at an incident angle of 85° exhibits the best catalytic activity and sensitivity to hydrogen peroxide (H_2O_2). This could be attributed to its largest contact area with the electrolyte. An effective approach is thus proposed to fabricate TiN nanostructure as H_2O_2 sensor by OAD.

Keywords: Titanium nitride; Nanostructure; Oblique angle deposition technique; Hydrogen peroxide; Sensor

Background

Nanostructured electrodes have stimulated great interests due to their potential applications in the areas of online real-time analysis and sensitive detection [1,2]. To meet the demand in those applications, electrodes need to have some important criteria including large specific area, high electrochemical activity, and good biocompatibility. In recent years, nanorod arrays directly grown on a current collector have been investigated as nanostructured electrodes for biosensor application since their well-defined one-dimensional (1D) structure is favorable for electron conducting and ion accessing [3]. Due to the exceptional combination of chemical, physical, mechanical, and electrical properties, titanium nitride (TiN) attracts much attention for their potential application in various fields such as protective coating [4], supercapacitors [5], and catalysis [6,7]. Recent literature has also reported its potential use as electrodes for pH sensor [8] and hydrogen peroxide (H_2O_2) sensor [3]. H_2O_2 is not only a byproduct of a wide range of biological processes but also an essential mediator in food, pharmaceutical, clinical, industrial, and environment analysis [9]. Therefore, it is of great importance to achieve sensitive and accurate determination of H_2O_2. TiN nanorod arrays (NRAs) are expected to possess good conductivity and biocompatibility with unique 1D nanostructure, making a superb electrode for H_2O_2 sensor.

The TiN NRAs can be obtained by a great number of methods, such as electrospinning [10] and solvent-thermal synthesis [3]. However, all the aforementioned methods need a nitridation treatment of TiO_2 nanorods in ammonia atmosphere at a high temperature. Therefore, a facile and one-step fabrication method to prepare TiN NRAs is in demand. Oblique angle deposition (OAD) technique is an electron beam evaporation method, which has been used in the industry for fabricating one- or two-dimensional materials at large-scale production with relatively low cost. It provides a simple way to produce large area, uniformly aligned nanorods with controlled porosity. During the OAD process, the vapor flux is deposited onto a substrate at a large angle α with respect to the substrate normal, and a well-aligned and separated nanorod arrays can be obtained due to the self-shadowing effect [11,12], with growth orientation toward the vapor flux direction [13]. Moreover, the porosity can be readily tuned by varying the oblique angle, and various substrates such as glass, F-doped SnO_2 (FTO), Si, etc., could be deposited on.

In this work, we report a one-step method, i.e., by OAD method using electron beam evaporation for fabricating TiN nanostructure with tunable morphologies and porosities. The TiN nanostructures are used as the electrodes for electrochemical sensing H_2O_2, exhibiting good performance.

* Correspondence: zjzhang@tsinghua.edu.cn
[3]Key Laboratory of Advanced Materials (MOE), School of Materials Science and Engineering, Tsinghua University, Beijing 100084, China
Full list of author information is available at the end of the article

Springer

Methods

Fabrication of TiN films by OAD

The TiN NRAs were deposited on silicon and FTO substrates using OAD described elsewhere [14]. The substrates were sequentially cleaned in acetone and alcohol by ultrasonic washer and then rinsed in deionized water for 5 min each. The system was pumped down to a base pressure of 2×10^{-5} Pa, and then the TiN films were deposited at a deposition rate of 0.5 nm s^{-1}, which was monitored by a quartz crystal microbalance. The deposition angle of TiN flux was set at *ca.* 0°, 60°, 70°, 80°, and 85° with respect to the substrate normal, respectively. The substrate temperature was maintained at *ca.* −20°C with liquid nitrogen.

Characterizations

The crystal structure of the TiN films was characterized by X-ray diffraction (XRD Rigaku 2500, Shibuya-ku, Japan), which was conducted from 20° to 60° at a scanning speed of 6° min^{-1}, using Cu Kα radiation (λ = 0.15406 nm). The morphology was characterized with a field emission scanning electron microscopy (SEM JEOL-7001 F, Akishima-shi, Japan) working at 20 kV. The microstructures of the prepared samples were characterized in detail with a transmission electron microscope (TEM JEOL-2010 F). The refractive index (n_e) of the TiN films deposited at various oblique angels was measured by spectroscopic ellipsometry (J.A. Woollam, Co., Inc., Lincoln, NE, USA).

Electrochemical measurements were carried out in a 250-mL quartz cell connected to an electrochemistry workstation (CHI 660, Shanghai Chenhua Instrument, Shanghai, China). A three-electrode assembly was adopted for the test, with the TiN films as a working electrode, a Pt foil as a counter electrode, a saturated Ag/AgCl as a reference electrode, and phosphate buffer solution (PBS, pH 7.0) as the electrolyte. The current versus time was recorded at −0.2 V bias versus saturated Ag/AgCl.

Results and discussion

Figure 1 shows the typical growth morphology of the TiN films deposited at various deposition angles. In the same deposition time of 30 min, the thickness of film gradually decreases from 860 to 190 nm as the deposition angle increases from 0° to 85°. It is because that the incident flux accepted by the substrate within a certain deposition time decreases at larger deposition angle [12]. The film morphology is obviously dependent on the oblique angle. For the film deposited at 0°, i.e., vertically deposited, a dense and flat surface was obtained as shown in Figure 1a. When the deposition angle was ≥60°, porous nanostructure was formed as shown in Figure 1b,c,d,e. It has been illustrated that during the OAD process, self-shadowing effect and limited surface diffusion lead to the formation of distinct
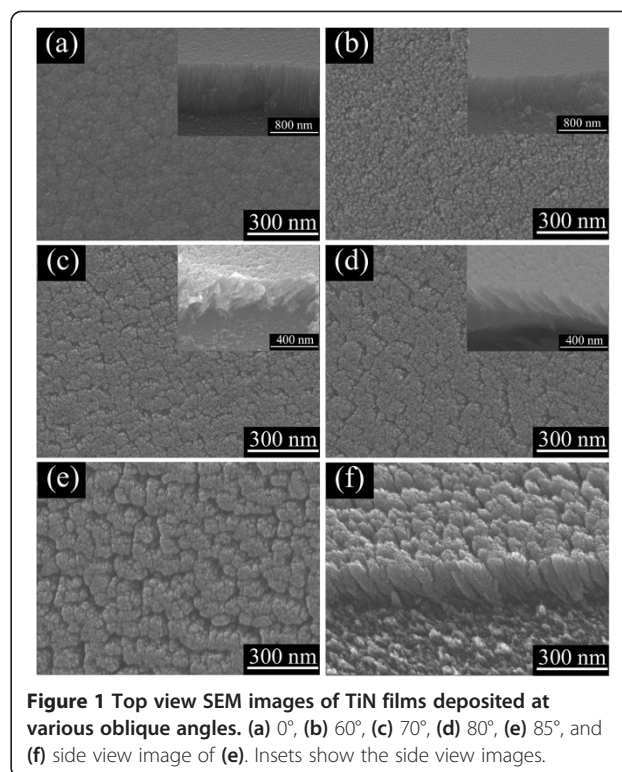

Figure 1 Top view SEM images of TiN films deposited at various oblique angles. (a) 0°, **(b)** 60°, **(c)** 70°, **(d)** 80°, **(e)** 85°, and **(f)** side view image of **(e)**. Insets show the side view images.

columnar structure [11,15]. With the deposition angle further increased to 85°, an aligned self-standing TiN nanorod arrays with length of *ca.* 270 nm and diameter of *ca.* 90 nm was obtained, which can be seen from the side view image in Figure 1f.

Figure 2 displays the XRD patterns of the TiN films deposited at various incident angles. It can be seen that the TiN film deposited at 0° exhibits (111) and (200) diffraction of the face-centered cubic (FCC) structure of TiN (JCPDS 38−1420). The (111) peak becomes weaker
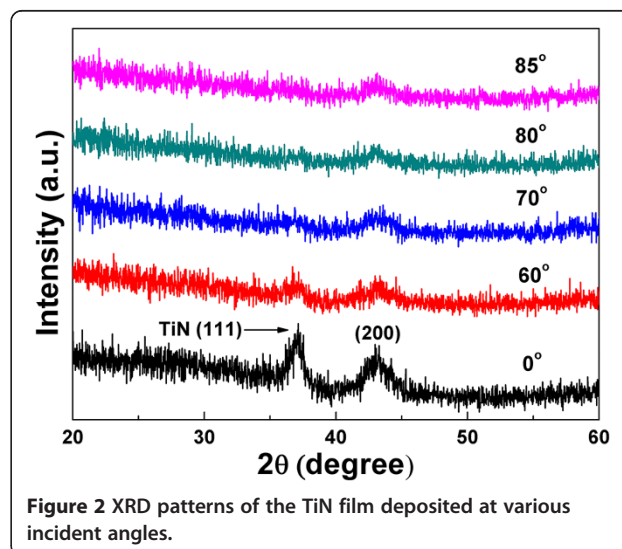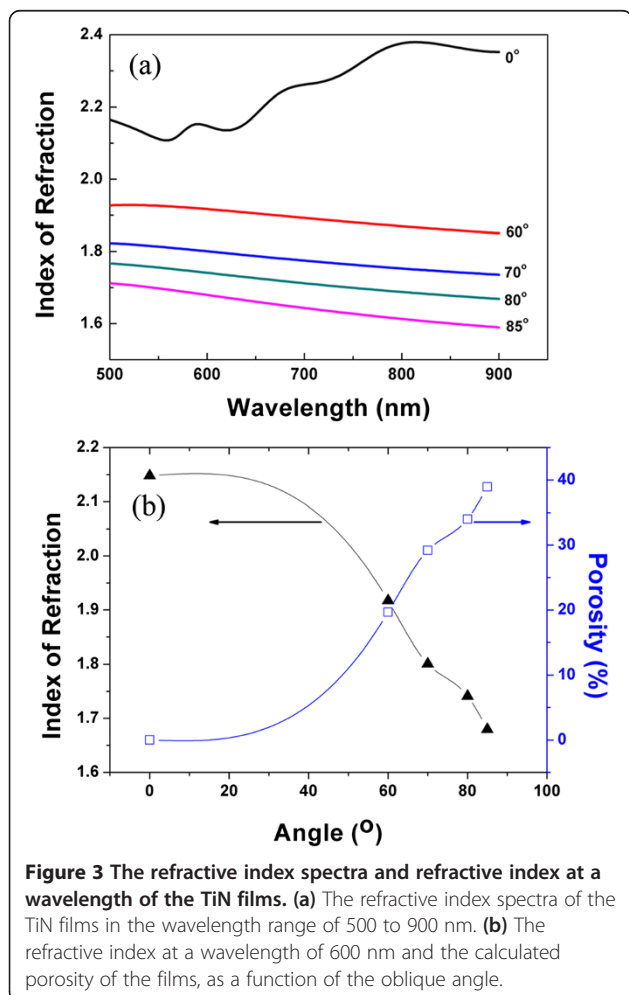

Figure 2 XRD patterns of the TiN film deposited at various incident angles.

for the films deposited at ≥60°, which can be attributed to the decrease in film thickness [16] and the formation of nanostructure during the OAD process.

The refractive index (n_e) of the as-prepared TiN films was measured by spectroscopic ellipsometry at wavelengths from 500 to 900 nm. Figure 3a plots the refractive index of the TiN film as a function of the wavelength. One can see that the film refractive index diminishes with the increase of the deposition angle. For a clear demonstration, we plot the variation of n_e at 600 nm as a function of the deposition angle, which is illustrated in Figure 3b. As the deposition angle increases from 0° to 85°, n_e decreases from 2.15 to 1.68, which is the result of the formation of nanostructure [17]. For two non-absorbing components with volume fractions f_i and refractive indices n_i, the Bruggemann effective medium approximation gives [18]

$$f_1\left[\left(n_1{}^2 - n_e{}^2\right)/\left(n_1{}^2 + 2n_e{}^2\right)\right] + f_2\left[\left(n_2{}^2 - n_e{}^2\right)/\left(n_2{}^2 + 2n_e{}^2\right)\right] = 0.$$

Figure 3 The refractive index spectra and refractive index at a wavelength of the TiN films. (a) The refractive index spectra of the TiN films in the wavelength range of 500 to 900 nm. **(b)** The refractive index at a wavelength of 600 nm and the calculated porosity of the films, as a function of the oblique angle.

Herein, n_e of a porous film is given by an average of air and material when the pore size is much smaller than the wavelength. Using the n_e at 600 nm, the porosity of the above TiN films is calculated using the Bruggemann approximation, and the result is displayed in Figure 3b. When the deposition angle is increased, the porosity increases and reaches the maximum at the deposition angle of 85°, which is in accordance with that observed by SEM (see Figure 1).

Figure 4a,b,c,d,e presents the cyclic voltammograms (CVs) of these TiN films in the absence and presence of H_2O_2 in 0.2 M PBS with pH 7.0. The reduction current increases with the addition of 3 mM H_2O_2, indicating an obvious catalytic reduction of H_2O_2 on the electrode [3]. Generally, the current difference, ΔI [($\Delta I = I$ (presence of H_2O_2) – I_0 (absence of H_2O_2)] at –0.2 V is adopted as a key index to evaluate the sensitivity for H_2O_2 [19], (ΔI reflects the sensitivity of detecting H_2O_2) Accordingly, ΔI is plotted as a function of the deposition angle in Figure 4f, where the ΔI in the unit of microampere per milligram has been normalized to the sample weight. It can be seen that ΔI increases dramatically with the increase of deposition angle, and the film deposited at 85° shows the best performance, whose current is more than twice as high as that of the film deposited at 0°. The current enhancement is attributed to the significant increase in contact area between the electrode and the electrolyte, which is verified by the aforementioned SEM morphology and porosity estimation.

In addition, TEM is employed to further study the microstructure of the TiN film deposited at 85°, which is served as a representative sample. From the low-magnification TEM image as shown in Figure 5a, one can see that the nanorod structure is clearly observed with length of *ca.* 280 nm and diameter of *ca.* 100 nm, which is in agreement with the SEM results (see Figure 1f). The nanorod exhibits a pine needle structure, which may lead to higher specific surface area than that of the nanorod with smooth or uniform surface. The TiN nanorod with high specific surface area may improve the performance in the process of H_2O_2 detection. Figure 3b displays the high-resolution TEM (HRTEM) image of the as-prepared TiN NRAs. The TiN crystalline grains can be seen clearly with the interplanar lattice spacing of 0.243 and 0.212 nm, corresponding well with that of (111) and (200) plane, respectively. The inset is the corresponding electron diffraction pattern, showing diffraction rings of (111) and (200) planes, which further supports the results of the XRD and HRTEM.

The current response of TiN NRAs by successively adding different concentration H_2O_2 was investigated in the PBS (pH 7), and –0.2 V was selected as the applied potential. The current has a good linear relationship with the H_2O_2 concentration which is in the range of 2.0×10^{-5} to 3.0×10^{-3} M. The regression equation is $y = 3.996x + 5.299$
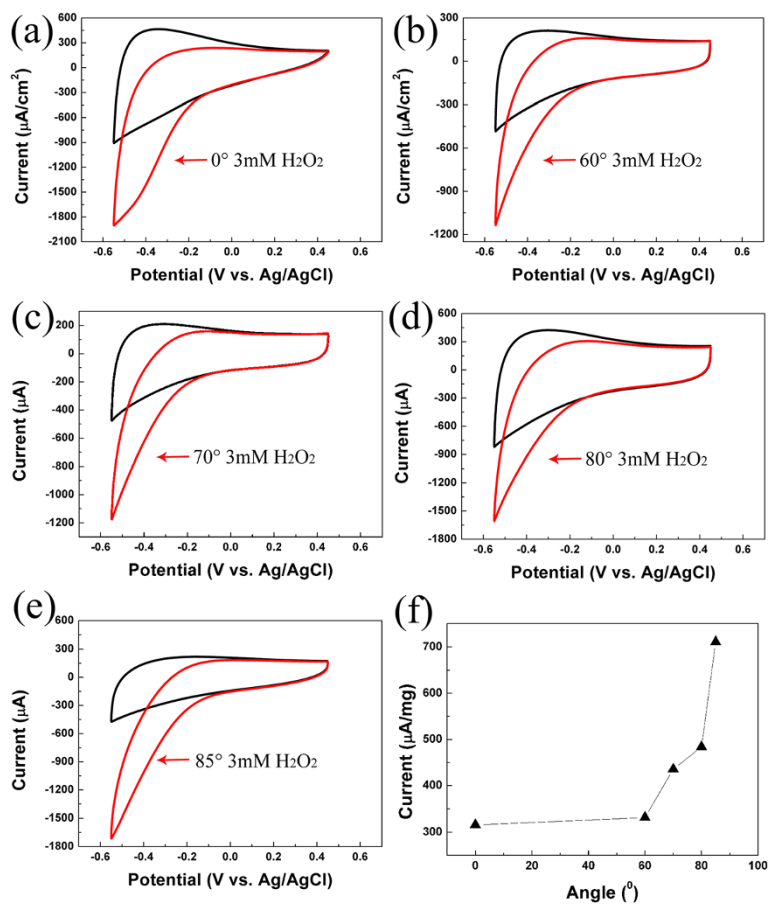
Figure 4 The C-V curve before and after adding 3 mM H$_2$O$_2$ for TiN films deposited at various angles. (a) 0°, **(b)** 60°, **(c)** 70°, **(d)** 80°, **(e)** 85°, and **(f)** the relationship of ΔI versus deposition angles.

($r = 0.9930$), as shown in Figure 6. Ascorbic acid (AA) is often an interference for hydrogen peroxide biosensors [20]. However, in our experiment, no interference was observed after adding 3 mM AA as shown in the inset of Figure 6. When solution of 3 mM H$_2$O$_2$ was added into the PBS, the reductive current increases rapidly and soon reaches stability. These results confirm that the TiN film deposited at the deposition angle of 85° possesses efficient electrocatalytic activity toward H$_2$O$_2$, which provides a
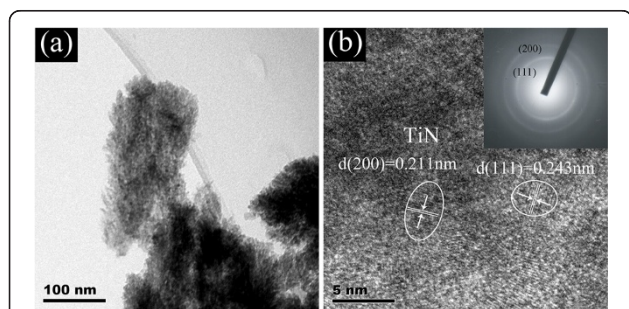

Figure 5 Low-resolution TEM image (a) and high-resolution TEM of the TiN deposited at oblique angle of 85° (b).
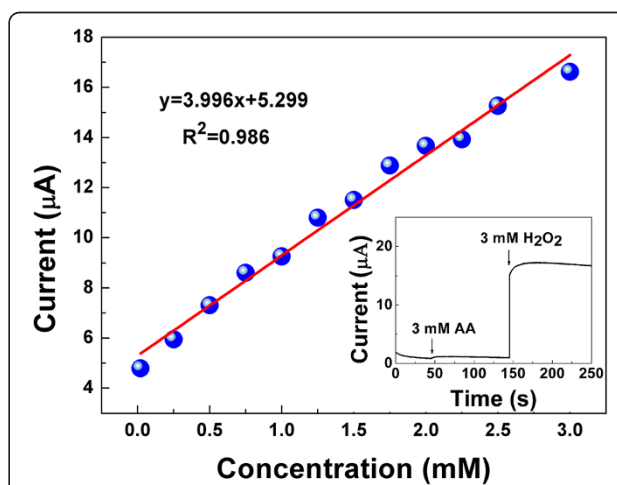

Figure 6 The linear relationship between current and the concentrate of H$_2$O$_2$. Inset is the current versus time after adding AA and H$_2$O$_2$.

promising way for fabricating sensors of detecting H_2O_2. However, compared with others' works [3,21,22], the catalytic efficiency for H_2O_2 of the TiN NRAs electrode is not very high. Further work is in need to improve the catalytic activity and sensitivity, such as increasing the length of TiN NRAs and enhancing the specific surface by modifying the OAD parameters.

Conclusions

TiN films with tunable porosity were fabricated by oblique angle deposition at different deposition angles. The porosity increases with the increase of the deposition angle due to the self-shadowing effect. All the TiN films show sensitive electrochemical catalytic property towards H_2O_2. The film of self-standing nanorods was obtained at the deposition angle of 85° and exhibits the best performance due to its highest porosity thus the largest effective contact area with the electrolyte. Therefore, oblique angle deposition provides a promising way to fabricate TiN nanostructure as a H_2O_2 sensor.

Competing interests
The authors declare that they have no competing interests.

Authors' contributions
ZX carried out the fabrication and characterization of the study and drafted the manuscript. XL participated in the design and coordination of the study. WW participated in the design and preparation and analyzed the results. CL participated in the design and preparation, analyzed the results, and helped draft the manuscript. ZL and ZZ participated in the design and coordination of the study. All authors read and approved the final manuscript.

Author details
[1]State Key Laboratory of New Ceramics and Fine Processing, School of Materials Science and Engineering, Tsinghua University, Beijing 100084, China. [2]High-Tech Institute of Xi'an, Xi'an, Shannxi 710025, China. [3]Key Laboratory of Advanced Materials (MOE), School of Materials Science and Engineering, Tsinghua University, Beijing 100084, China.

References
1. Njagi J, Chernov MM, Leiter J, Andreescu S: **Amperometric detection of dopamine in vivo with an enzyme based carbon fiber microbiosensor.** *Anal Chem* 2010, **82**:989–996.
2. Jiang LC, Zhang WD: **Electrodeposition of TiO2 nanoparticles on multiwalled carbon nanotube arrays for hydrogen peroxide sensing.** *Electroanalysis* 2009, **21**:988–993.
3. Dong S, Chen X, Gu L, Zhang L, Zhou X, Liu Z, Han P, Xu H, Yao J, Zhang X: **A biocompatible titanium nitride nanorods derived nanostructured electrode for biosensing and bioelectrochemical energy conversion.** *Biosens Bioelectron* 2011, **26**:4088–4094.
4. Starosvetsky D, Gotman I: **TiN coating improves the corrosion behavior of superelastic NiTi surgical alloy.** *Surf Coat Technol* 2001, **148**:268–276.
5. Lu X, Wang G, Zhai T, Yu M, Xie S, Ling Y, Liang C, Tong Y, Li Y: **Stabilized TiN nanowire arrays for high-performance and flexible supercapacitors.** *Nano Lett* 2012, **12**:5376–5381.
6. Musthafa OM, Sampath S: **High performance platinized titanium nitride catalyst for methanol oxidation.** *Chem Commun* 2008:67–69.
7. Nunes Kirchner C, Hallmeier KH, Szargan R, Raschke T, Radehaus C, Wittstock G: **Evaluation of thin film titanium nitride electrodes for electroanalytical applications.** *Electroanalysis* 2007, **19**:1023–1031.
8. Wang Y, Yuan H, Lu X, Zhou Z, Xiao D: **All solid-state pH electrode based on titanium nitride sensitive film.** *Electroanalysis* 2006, **18**:1493–1498.
9. Schreier TM, Rach JJ, Howe GE: **Efficacy of formalin, hydrogen peroxide, and sodium chloride on fungal-infected rainbow trout eggs.** *Aquaculture* 1996, **140**:323–331.
10. Sun D, Lang J, Yan X, Hu L, Xue Q: **Fabrication of TiN nanorods by electrospinning and their electrochemical properties.** *J Solid State Chem* 2011, **184**:1333–1338.
11. Vick D, Friedrich L, Dew S, Brett M, Robbie K, Seto M, Smy T: **Self-shadowing and surface diffusion effects in obliquely deposited thin films.** *Thin Solid Films* 1999, **339**:88–94.
12. Dolatshahi-Pirouz A, Hovgaard MB, Rechendorff K, Chevallier J, Foss M, Besenbacher F: **Scaling behavior of the surface roughness of platinum films grown by oblique angle deposition.** *Phys Rev B* 2008, **77**:115427.
13. Wolcott A, Smith WA, Kuykendall TR, Zhao Y, Zhang JZ: **Photoelectrochemical water splitting using dense and aligned TiO2 nanorod arrays.** *Small* 2009, **5**:104–111.
14. Xie Z, Zhang Y, Liu X, Wang W, Zhan P, Li Z, Zhang Z: **Visible light photoelectrochemical properties of N-Doped TiO 2 nanorod arrays from TiN.** *J Nanomater* 2013, **2013**.
15. Dohnalek Z, Kimmel GA, Ayotte P, Smith RS, Kay BD: **The deposition angle-dependent density of amorphous solid water films.** *J Chem Phys* 2003, **118**:364.
16. Zhao J, Wang X, Chen Z, Yang S, Shi T, Liu X: **Overall energy model for preferred growth of TiN films during filtered arc deposition.** *J Phys D Appl Phys* 1997, **30**:5.
17. Ni J, Zhu Y, Wang S, Li Z, Zhang Z, Wei B: **Nanostructuring HfO2 thin films as antireflection coatings.** *J Am Ceram Soc* 2009, **92**:3077–3080.
18. Ho PK, Stephen D, Friend RH, Tessler N: **All-polymer optoelectronic devices.** *Science* 1999, **285**:233–236.
19. Qian L, Yang X: **Composite film of carbon nanotubes and chitosan for preparation of amperometric hydrogen peroxide biosensor.** *Talanta* 2006, **68**:721–727.
20. Miao Y, Tan SN: **Amperometric hydrogen peroxide biosensor based on immobilization of peroxidase in chitosan matrix crosslinked with glutaraldehyde.** *Analyst* 2000, **125**:1591–1594.
21. Wang G, Xu J-J, Chen H-Y, Lu Z-H: **Amperometric hydrogen peroxide biosensor with sol–gel/chitosan network-like film as immobilization matrix.** *Biosens Bioelectron* 2003, **18**:335–343.
22. Liu Y, Chu Z, Jin W: **A sensitivity-controlled hydrogen peroxide sensor based on self-assembled prussian blue modified electrode.** *Electrochem Commun* 2009, **11**:484–487.